

# Gene Expression on DNA Biochips Patterned with Strand-Displacement Lithography

Günther Pardatscher, Matthaues Schwarz-Schilling, Shirley S. Daube, Roy H. Bar-Ziv, and Friedrich C. Simmel\*

**Abstract:** Lithographic patterning of DNA molecules enables spatial organization of cell-free genetic circuits under well-controlled experimental conditions. Here, we present a biocompatible, DNA-based resist termed “Bephore”, which is based on commercially available components and can be patterned by both photo- and electron-beam lithography. The patterning mechanism is based on cleavage of a chemically modified DNA hairpin by ultraviolet light or electrons, and a subsequent strand-displacement reaction. All steps are performed in aqueous solution and do not require chemical development of the resist, which makes the lithographic process robust and biocompatible. Bephore is well suited for multistep lithographic processes, enabling the immobilization of different types of DNA molecules with micrometer precision. As an application, we demonstrate compartmentalized, on-chip gene expression from three sequentially immobilized DNA templates, leading to three spatially resolved protein-expression gradients.

**P**atterned immobilization of functional biomolecules such as antibodies or aptamers onto solid substrates has already found a wide range of applications in high-throughput analytics and diagnostics.<sup>[1]</sup> Biochips are not only used in biosensing devices, but also as templates for tissue and organ engineering. Most of these applications require static and biocompatible secondary immobilization of biochemical analytes such as nucleic acids or proteins, or molecules that mediate the specific adhesion of cells.

Recently, lithographically structured DNA biochips have also been utilized in a dynamic context. Surface-immobilized DNA brushes have been used to study the biophysical properties of dense polyelectrolyte phases,<sup>[2]</sup> or to facilitate cell-free gene expression on a chip.<sup>[3]</sup> Compared to other cell-free synthetic biological systems that either operate in bulk<sup>[4]</sup> or utilize vesicles,<sup>[5]</sup> emulsion droplets,<sup>[6]</sup> or microfluidic reactors<sup>[7]</sup> as reaction compartments, chip-based systems have a variety of unique properties.

In gene brushes, DNA molecules are spatially localized but can be transcribed and translated into freely diffusing RNA and proteins, respectively.<sup>[8]</sup> RNA and proteins can be exchanged between separate brushes and thus establish spatially distributed in vitro gene circuits.<sup>[9]</sup> Lithographic structuring of the brushes enables control over local concentrations, directs the propagation of diffusive signals on the chip, and defines the timescale of signaling among spatially separated gene brushes.

In previous work on DNA brushes, the biocompatible lithography resist “Daisy”, which is based on a heterobifunctional polyethylene glycol (PEG) with a photoactive head-group,<sup>[8a]</sup> was used to immobilize DNA on silicon or glass. Other approaches towards photolithographic patterning of DNA have been developed previously, but none of these have been used in the context of cell-free gene expression. One of the methods involved cinnamate-based ultraviolet (UV) photo-crosslinking of DNA strands,<sup>[10]</sup> while a different method used DNA hairpins modified with a photocleavable group to spatially address gel-immobilized DNA circuits.<sup>[11]</sup> Another approach<sup>[12]</sup> based on photocleavable DNA utilized UV-induced destruction of single-stranded DNA “toehold” regions. These toeholds were used to attach functionalized DNA, resulting in a negative tone pattern transfer, in which only the non-exposed regions were functionalized.

For the present work, we combined the most beneficial features of the previous concepts into a novel approach for positive-tone multistep lithography of gene brushes, which we termed Biocompatible Electron- and PHOto-sensitive REsist (Bephore). The basic working principle of Bephore is illustrated in Figure 1a. Lithography was performed on a silicon chip with a 50 nm layer of silicon dioxide. To reduce unspecific adsorption of biomolecules to the surface, the oxide was silanized with a layer of biotinylated PEG (MW: 5000), which in turn allowed streptavidin-mediated attachment of a biotinylated, photosensitive DNA construct consisting of two strands. Only the biotinylated, photocleavable strand (PC strand, 53 nt) was tethered to the surface, while the second strand (PH, 30 nt) was hybridized to the PC strand. The DNA component of Bephore was specifically designed to result in a positive tone resist. To this end, the PC strand was engineered to consist of a stem region (40 nt), a single-stranded loop (5 nt), and a short sequence (8 nt) complementary to the stem. The photocleavable modification (based on a nitrophenyl moiety;<sup>[13]</sup> see Figure S1 in the Supporting Information) was placed in the loop region to avoid potential distortion of the DNA helix.

The complementary sequence was designed to form an 8 bp hairpin–stem duplex, which is stable enough to inhibit

[\*] G. Pardatscher, M. Schwarz-Schilling, Prof. Dr. F. C. Simmel  
Physics-Department and ZNN, Technische Universität München  
Am Coulombwall 4a, 85748 Garching (Germany)  
E-mail: simmel@tum.de

Dr. S. S. Daube, Prof. Dr. R. H. Bar-Ziv  
Department of Chemical and Biological Physics  
The Weizmann Institute of Science, Rehovot 76100 (Israel)

Supporting information and the ORCID identification number(s) for the author(s) of this article can be found under:  
<https://doi.org/10.1002/anie.201800281>.

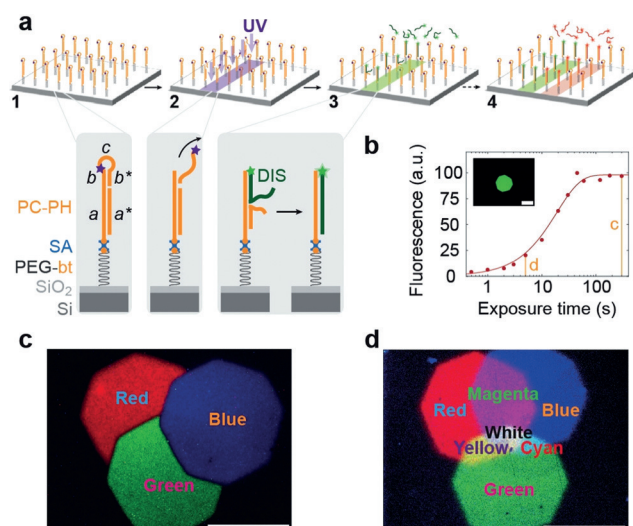


**Figure 1.** Lithographic patterning of Bephore. a) 1. A silicon (Si) chip with a layer of oxide ( $\text{SiO}_2$ ) is passivated by biotinylated polyethylene glycol (PEG-bt). Photosensitive and biotinylated DNA (strand PC with sequence domains  $abc b^*$ ) is linked to the surface via streptavidin (SA) and hybridized to another strand (PH; sequence  $a^*$ ). 2. Illumination of an area with UV light cuts the photocleavable linker in the PC strand, leaving a short toehold domain ( $b$ ) of PC single-stranded. 3. A fluorescently labeled DIS strand ( $b^* a^*$ ) can now hybridize to the PC strand through toehold-mediated displacement of the PH strand. 4. The lithography can be repeated to immobilize DIS strands with different labels. b) The surface density of immobilized DIS strands depends on the duration of UV exposure. The solid line represents a fitted model (Section 2 in the Supporting Information). The two orange lines indicate the exposure times used for (c) and (d). Inset: Microscopy image of DIS strands labeled with ATTO 532 fluorophores attached to an area previously illuminated with UV through a field iris diaphragm for 120 s. c, d) Three-step lithography allows the patterning of DIS strands labeled with red (AlexaFluor 647), green (ATTO 532), or blue (ATTO 425) fluorophores. Long exposure times yield areas filled exclusively with one type of DIS (c), and short exposures and overlapping regions result in mixed colors (d). Fluorescence images were colored and merged according to the RGB color model. Scale bars: 50  $\mu\text{m}$ .

toehold-mediated strand displacement of PH. Upon local illumination of the chip with UV light or electrons, the photoactive linker in the loop is cleaved, thereby opening the loop. The resulting shorter fragment of the PC strand is unstable and rapidly dissociates into solution, leaving a short, single-stranded toehold region on the PC strand. Next, a fluorescently labeled strand (DIS) was added, which hybridizes to the PC strand through toehold-mediated strand displacement of PH.<sup>[14]</sup> Areas with surface-bound DIS strands were then observed by fluorescence microscopy, where the fluorescence intensity correlates with the duration of the UV exposure (Figure 1 b).

For applications in cell-free gene expression, positive pattern transfer is preferred over an alternative negative-tone approach. Since photocleavage is incomplete even after long UV exposure times (Figure S2), negative-tone patterning would result in considerable DNA attachment to the background. Highly specific attachment of DNA only to patterned regions, however, is essential for structured on-chip gene circuits, since even a small amount of unspecifically bound

DNA would result in considerable spurious protein production.

To demonstrate the capacity of our approach for multistep lithography, we consecutively immobilized DIS strands labeled with red, green, or blue fluorophores through a stepwise repetition of UV illumination and incubation with the respective DIS strands. Depending on the UV exposure times, overlapping regions were filled either exclusively by a single type of DIS or by a mixture of the strands (Figure 1 c,d).

We further realized a precisely aligned, multistep lithographic process by mask projection (Figure 2), reproducing an expressionist painting as a miniaturized DNA-based replica. This underlines the multiplexing capability of Bephore, which may be used to precisely pattern multiple biomolecular fields with different functionalities in close proximity.

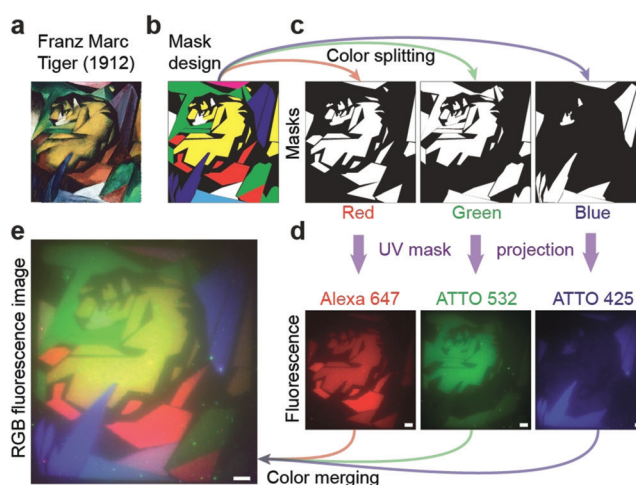


**Figure 2.** Mask-projection RGB lithography. a) The oil painting “Tiger” (1912) by Franz Marc served as a template for the lithographic process. b) We first simplified the picture and reduced the colors to RGB. c) From the resulting image we derived three masks, one for each lithography step. d) The masks were then consecutively projected onto a Bephore chip to immobilize the labeled DIS strands. e) Eventually, the three resulting fluorescence images were merged to give an approximately 4000 $\times$  miniaturized RGB version of the “Tiger”. Scale bars: 20  $\mu\text{m}$ .

In addition to photolithography, Bephore can be patterned with higher precision using electron-beam lithography. Since this technique does not require a mask and is not restricted by the diffraction limit of light, ebeam lithography is especially suited for fast prototyping of fine patterns with line widths on the order of around 100 nm.<sup>[15]</sup>

Figure 3 illustrates the attachment of DIS strands to areas or lines exposed to various electron doses (electrons per area or length). We hypothesize that in this case the photocleavable linker is activated by secondary electrons with kinetic energies (2–50 eV)<sup>[16]</sup> similar to the energy of UV photons (3.4 eV for a wavelength of 365 nm). The broad range of electron energies may explain the rapid degradation of the resist with increasing dose.

We finally investigated compartmentalized gene expression on a Bephore chip. We created a linear DNA template

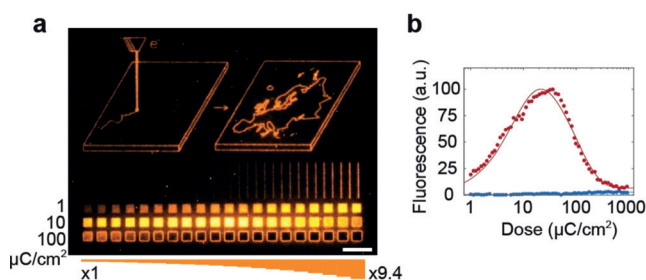


**Figure 3.** Electron-beam lithography with Bephore. a) Fluorescence image of an ebeam-patterned chip after incubation with DIS strands labeled with ATTO 532. Here, ebeam lithography was both applied to draw a schematic illustration of a beam-patterned geographical map of Europe on a chip (top), and to perform line and area dose tests (bottom; see also Figure S3). Numbers on the left show the dose used to write the first square in a row, bars at the bottom indicate the dose factors along the rows. b) Quantification of fluorescence intensities from area dose tests on a Bephore chip (red) and a similar chip without the photocleavable DNA as a control (blue). Solid lines represent a fitted model (Section 2 in the Supporting Information). Scale bar: 10  $\mu\text{m}$ .

coding for a fluorescent protein using polymerase chain reaction (PCR) such that the DNA has a fluorescent label on one end and a single-stranded DIS sequence on the other end (Figure S4). The gene was then immobilized on a chip at a density on the order of  $100 \mu\text{m}^{-2}$  (Section 1.4 of the Supporting Information), enclosed in a compartment, and expressed in a reconstituted gene expression system<sup>[17]</sup> or in cell extract from *E.coli*<sup>[18]</sup> (Figure 4a–c, Figure S5). A thin channel connects the chamber to a reservoir, which provides a continuous supply of expression system, amino acids, and nucleotides. Protein expression was then monitored using fluorescence microscopy, and a strong signal was measured in the compartment with a DNA pattern, while the control chamber remained dark (with only 2% of the intensity in the gene-brush chamber). Repeated protein expression from the same DNA brush proved that the DNA was not removed from the chip or strongly degraded.

To further demonstrate the potential of the system for the realization of spatially distributed genetic circuits on a chip, we applied multistep Bephore lithography to immobilize genes coding for three different fluorescent proteins. Figure 4e shows the corresponding gene brushes immobilized in separate reaction chambers on a chip. The brushes were transcribed and translated into the respective fluorescent proteins, and thus the reaction chambers acted as “sources” of the protein products. Consequently, concentration gradients of freely diffusing fluorescent proteins were established in the channels connecting the compartments (Figure 4f and Video S1).

In summary, we have developed a DNA-based resist for multistep lithography on biochips and demonstrated its use in compartmentalized gene expression from immobilized DNA templates. The resist is sensitive to UV light and electrons and hence allows the assembly of DNA brushes ranging in size from macroscopic dimensions down to brush widths on the order of 100 nanometers. The resist is based on commercially available components and the development-free lithography

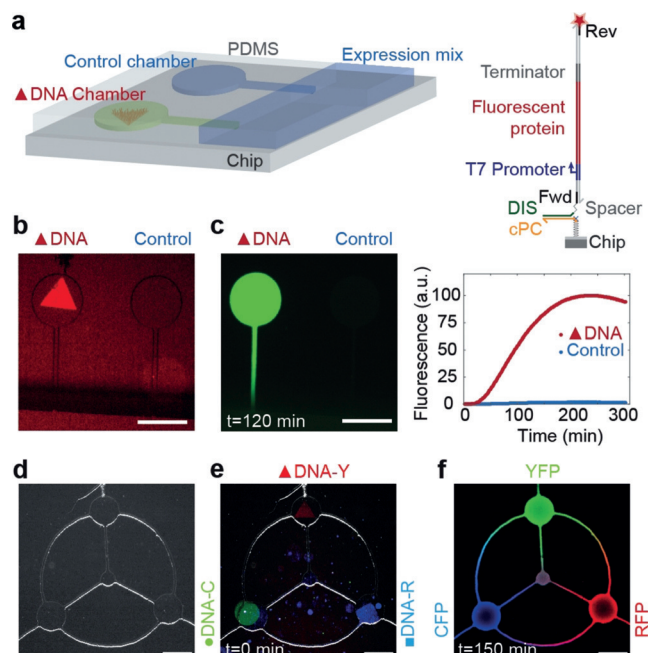


**Figure 4.** Compartmentalized gene expression. a) Illustration of a Bephore chip with a triangular region of immobilized DNA coding for a fluorescent protein. The DNA is enclosed in a compartment fabricated from polydimethylsiloxane (PDMS); a second chamber without DNA acts as a negative control. Channels (20  $\mu\text{m}$  in width) connect the compartments to a large reservoir of cell-free expression system to allow sustained expression. Right: To bind a gene to Bephore, it was labeled with a fluorophore and a single-stranded DIS sequence through PCR with modified primers Rev and Fwd. DIS and Fwd were separated by a triethylene glycol spacer. b) Fluorescence image of an immobilized gene coding for the yellow fluorescent protein YPet (1.7 kbp DNA labeled with AlexaFluor 647). c) Gene expression in the PURExpress system was monitored in fluorescence microscopy. The chamber with the triangular DNA region showed a clear signal, while the control chamber remained dark. Without the addition of fresh expression mix to the reservoir, the reaction terminated after a few hours. d) A bright-field image of three chambers connected by channels (see Figure S6), in which DNA brushes coding for cyan (DNA-C, 1 kbp, ATTO 532), yellow (DNA-Y, 1.7 kbp, Alexa Fluor 647) and red (DNA-R, 1.8 kbp, ATTO 425) fluorescent proteins were immobilized. Panel (e) shows a colored overlay of the fluorescence images of the DNA brushes at the beginning of gene expression ( $t=0 \text{ min}$ ) with the bright-field image. f) Overlay image of cyan (mTurquoise2), yellow (YPet) and red (mScarlet) fluorescent proteins after 150 min of expression. Scale bars: 300  $\mu\text{m}$ .

process in aqueous solution ensures compatibility with a wide range of biomolecular agents.

As indicated in this work, Bephore can be readily used for the spatial organization of cell-free gene expression reactions, thereby enabling the precise engineering of synthetic gene circuits for chip-based artificial cells. The multiplexing capabilities of Bephore may find further use in biomedical diagnostics or biomaterials applications.

## Acknowledgements

This project was generously funded by the Volkswagen Stiftung (grant no. 89 883/89 884). M.S.-S. gratefully acknowl-

edges support by the DFG through the GRK 2062. We thank Aurore Dupin and Ludwig Bauer for providing plasmid DNA and the protein GamS.

### Conflict of interest

The authors declare no conflict of interest.

**Keywords:** DNA biochips · electron-beam lithography · polymer brushes · photolithography · synthetic biology

**How to cite:** *Angew. Chem. Int. Ed.* **2018**, *57*, 4783–4786  
*Angew. Chem.* **2018**, *130*, 4873–4876

- 
- [1] J. D. Hoheisel, *Nat. Rev. Genet.* **2006**, *7*, 200–210.
- [2] a) D. Bracha, E. Karzbrun, G. Shemer, P. A. Pincus, R. H. Bar-Ziv, *Proc. Natl. Acad. Sci. USA* **2013**, *110*, 4534–4538; b) D. Bracha, E. Karzbrun, S. S. Daube, R. H. Bar-Ziv, *Acc. Chem. Res.* **2014**, *47*, 1912–1921; c) D. Bracha, R. H. Bar-Ziv, *J. Am. Chem. Soc.* **2014**, *136*, 4945–4953.
- [3] A. Buxboim, S. S. Daube, R. Bar-Ziv, *Mol. Syst. Biol.* **2008**, *4*, 181.
- [4] a) J. Kim, K. S. White, E. Winfree, *Mol. Syst. Biol.* **2006**, *2*, 0; b) K. Montagne, R. Plasson, Y. Sakai, T. Fujii, Y. Rondelez, *Mol. Syst. Biol.* **2011**, *7*, 466.
- [5] F. Caschera, J. Lee, K. K. Y. Ho, A. P. Liu, M. C. Jewett, *Chem. Commun.* **2016**, *52*, 5467–5469.
- [6] M. Weitz, J. Kim, K. Kapsner, E. Winfree, E. Franco, F. C. Simmel, *Nat. Chem.* **2014**, *6*, 295–302.
- [7] H. Niederholtmeyer, V. Stepanova, S. J. Maerkl, *Proc. Natl. Acad. Sci. USA* **2013**, *110*, 15985–15990.
- [8] a) A. Buxboim, M. Bar-Dagan, V. Frydman, D. Zbaida, M. Morpurgo, R. Bar-Ziv, *Small* **2007**, *3*, 500–510; b) Y. Heyman, A. Buxboim, S. G. Wolf, S. S. Daube, R. H. Bar-Ziv, *Nat. Nanotechnol.* **2012**, *7*, 374–378.
- [9] a) E. Karzbrun, A. M. Tayar, V. Noireaux, R. H. Bar-Ziv, *Science* **2014**, *345*, 829–832; b) A. M. Tayar, E. Karzbrun, V. Noireaux, R. H. Bar-Ziv, *Nat. Phys.* **2015**, *11*, 1037–1041; c) A. M. Tayar, E. Karzbrun, V. Noireaux, R. H. Bar-Ziv, *Proc. Natl. Acad. Sci. USA* **2017**, *114*, 11609–11614.
- [10] L. Feng, J. Romulus, M. Li, R. Sha, J. Royer, K.-T. Wu, Q. Xu, N. C. Seeman, M. Weck, P. Chaikin, *Nat. Mater.* **2013**, *12*, 747–753.
- [11] S. M. Chirieleison, P. B. Allen, Z. B. Simpson, A. D. Ellington, X. Chen, *Nat. Chem.* **2013**, *5*, 1000–1005.
- [12] F. Huang, H. Xu, W. Tan, H. Liang, *ACS Nano* **2014**, *8*, 6849–6855.
- [13] J. Olejnik, S. Sonar, E. Krzymańska-Olejnik, K. J. Rothschild, *Proc. Natl. Acad. Sci. USA* **1995**, *92*, 7590–7594.
- [14] B. Yurke, A. J. Turberfield, A. P. Mills, F. C. Simmel, J. L. Neumann, *Nature* **2000**, *406*, 605–608.
- [15] G. Pardatscher, D. Bracha, S. S. Daube, O. Vonshak, F. C. Simmel, R. H. Bar-Ziv, *Nat. Nanotechnol.* **2016**, *11*, 1076–1081.
- [16] M. A. McCord, M. J. Rooks, *Handbook of Microlithography, Micromachining, and Microfabrication, Vol. 1* (Ed.: P. Rai-Choudhury), SPIE, **1997**.
- [17] Y. Shimizu, A. Inoue, Y. Tomari, T. Suzuki, T. Yokogawa, K. Nishikawa, T. Ueda, *Nat. Biotechnol.* **2001**, *19*, 751–755.
- [18] Z. Z. Sun, C. A. Hayes, J. Shin, F. Caschera, R. M. Murray, V. Noireaux, *J. Vis. Exp.* **2013**, 50762.

Manuscript received: January 8, 2018

Accepted manuscript online: February 22, 2018

Version of record online: March 15, 2018